HYPERSPECTRAL IMAGE ANALYSIS FOR MINERAL EXPLORATION IN BADUSH REGION OF IRAQ

Sayyad S. B.[1], Mohammed Z. R.[1], Deshmukh R. R.[2]
[1]Milliya Arts, Science & Management Science College, Beed (MS) India -431122
[2]Department of Computer Science & IT, Dr. Babasaheb Ambedkar Marathwada University, Aurangabad (MS) India -431001
E-mail: syedsb@rediffmail.com, zeeeshan.shaikh@gmail.com, rrdeshmukh.csit@bamu.ac.in

KEY WORDS: Hyperspectral imaging, minimum noise fraction, pixel purity index.

ABSTRACT: The absorptions in visible, near and short wave infrared is an effective region for mineral identification and mapping. This paper reports the mineral identification using Hyperion data set over part of Badush area from Iraq. Removal of bad bands and bad columns were performed. The data is converted from radiance to reflectance and to remove the atmospheric effects we have used the fast line of sight atmospheric absorptions for hyper cube (FLAASH). Noise and spectral dimensionality reduction using minimum noise fraction transform from which few bands have been considered as noise free bands. Pixel purity index (PPI) for spatial dimensionality reduction and few hundred spectrally pure pixels were taken into account. The n-dimensional visualizer used to locate and group the purest pixels for end member extraction. The cluster of end members is identified by comparing the spectra with the available United State Geological Survey (USGS) spectral library. The end members are used for classification using spectral angle mapper algorithm which helps to discriminate and identify the occurrences of the same minerals. The area from Iraq is considered for study which shows the potential of remotely sensed data where the areas are extremely inaccessible in other ways. The study reveals the feasibility and potential of hyperspectral data in mineral exploration.

1. INTRODUCTION

The hyperspectral remote sensing or Imaging spectroscopy is one of the popular approach in surface mineral identification and abundance mapping. The hyperspectral sensor captures the information from the focused area in many narrow contiguous bands which provides the detailed information about the underlying area with fine spectral and spatial resolution as compared to multi spectral remote sensed data. Materials absorb radiation at particular wavelengths which helps to identify features based on the position of absorption within the spectrum and each feature has its unique signature which helps to uniquely identify different features. The uniqueness is because when the electromagnetic radiation interacts with the atoms and molecules which cause charge transfer and electronic transition to higher energy levels which creates absorption features in the reflectance spectrum. The hyperspectral remote sensing provides a good opportunity in mineral identification. The light reflects by the surface is directly depends on the composition and the crystallographic structure. Different minerals have unique absorptions across the electromagnetic spectrum which creates unique spectral signature for each mineral. With the help of hyperspectral remote sensing, the wide range of minerals can be remotely identified like sulphates iron oxides, , mica, chlorites, clays amphiboles, talc, carbonates, quartz, garnets, pyroxenes, olivine, feldspars and, as well as their physicochemistries such as the cation composition and long and short range order. S.S.S., Upadhyay et.al (2012) reported each of the minerals have their unique reflectance and absorption pattern across different wave-length which helps to identify the minerals uniquely. In this work we have used hyperspectral image to analyse by applying different standard algorithm to extract the information for mineral identification.

2. DATASET

The Hyperion data onboard EO-1 satellite was obtained from Earth explorer website which was acquired on 16 November 2008 is used for this study. The Hyperion Level 1R data, which is radiometrically corrected and geometrically mapped is used for the current study. The Hyperion sensor collects 242 unique spectral bands ranging from 0.35 to 2.5 micrometers having a 10 nm bandwidth. There are three types of data available these are L1R, L1T and level 1Gst which is radiometrically and geometrically corrected data. It is also terrain corrected. This dataset is having same details as level1R data. It was used for geometric correction of L1R data. The study area is a part of

Badush village which is located in the northern region of Iraq The area is located at northwest of Mosul City covering a part of Badush. The area is located at 36° 52’ 32” N and 43° 3’ 36”E.

Figure: 1 Hyperion data of study area (Badush, Iraq)

3. METHODS

The ENVI 5.3 software was used for entire image processing operations. The following section contains the set of operations which were performed on the data set.

3.1 Data Preprocessing

The dataset has to be corrected for bad bands, striping effects and smiling effects in the dataset before the atmospheric correction. Pre-processing of hyperspectral images is required for removing sensor errors during the acquisition process. The Hyperion sensor records the data in 220 narrow continuous band out of which some bands were identified as bad bands because some bands are not illuminated and some bands corresponds to low sensitive material of the spectrometer. Finally we have derived a spectral subset of 190 bands which is considered for further processing. After the bad band removal the data was searched for bad columns and band by band the bad column removal was done.

3.2 Atmospheric correction

The absorption and scattering of the solar radiance takes place when it interacts with the atmosphere and the radiance reaches the sensor contains the effect of atmospheric absorption and also dominated by solar irradiance curve. To compensate with these atmospheric effects atmospheric correction is required before further processing the dataset. There are various approaches for atmospheric correction is available like Empirical approach to get relative reflectance and atmospheric models to get absolute reflectance. In the present work we have used fast line

of sight atmospheric analysis of spectral hypercube (FLAASH) atmospheric correction tool is used to remove errors from the bands in the visible range through NIR and SWIR regions, and it converts the DN value into ground spectral reflectance. FLAASH accepts radiance image as a input which is having calibrated radiance data in a long integer, floating point or integer data types. The image should have BIL (band interleaved by line) or BIP(band interleaved by pixel) formats. To convert the raw image into radiance units all the VNIR bands should be divided by 400 the SWIR bands by 800. A plain text file called scale factor file containing array of 400.0 for first 68 VNIR bands and 800.0 for the 170 SWIR bands was created and used at the time of inputting the image in FLAASH. After performing atmospheric correction spectral and spatial dimensionality reduction is done using minimum noise fraction and pixel purity index and few hundred purest pixel were identified and end members were extracted which is compared with the USGS standard library. Spectral angle mapper and spectral feature fitting algorithm were used for classification.

3.3 Minimum noise fraction transform

The minimum noise fraction (MNF) transformation is used to reduce the dimensionality of the data. In which it determines the inherent dimensionality of image data, to segregate noise in the data, and to reduce the computational requirements for subsequent processing [Boardman, J.W. et. al 1994]. The minimum noise fraction (MNF) transformation actually has two rotations of PCA. This is a two-step process. The first step results in transformed data in which the noise has unit variance matrix and no band-to-band correlations. The second step is a standard Principal Components transformation of the noise-whitened data [Green, A.A. 1985].the transform orders the data according to the signal to noise ratio. In the present work MNF image was created for the spectral subset of 196 bands out of which 20 bands were considered to be noise free according to their Eigen values and these small number of noise free bands were considered for further processing.

3.4 Pixel purity index (PPI)

The pixel purity Index (PPI) applied on the image obtained from minimum noise fraction transform which was used to find out the most spectrally pure or extreme pixels in multispectral and hyperspectral images [Boardman, J. W. 1995]. The most spectrally pure pixels typically correspond to mixing end members. PPI is computed by repeatedly projecting n-dimensional scatter plots onto a random unit vector. ENVI records the extreme pixels in each projection are recorded-those pixels that fall onto the ends of the unit vector and it record the total number of times each pixel is marked as extreme. A PPI image is created where each pixel value corresponds to the number of times that pixel was recorded as extreme. PPI was calculated with 10000 iterations and a threshold factor in the data unit was set to 3 for extreme pixel selection. The threshold should be higher minimum threshold so that only few hundred purest pixels will be considered for the end member extraction. The results of the PPI are used as input into n-D Visualizer

3.5 The n-dimensional visualizer

The output PPI image which is actually a spatial subset of the purest pixels is used in the n-dimensional visualizer to visualize the purest pixels as a points in n dimensions and to make the cluster of the pixels which probably belongs to a same class by examining their spectral reflectance and these pixels mostly projected on the corners of the scatter plot. From these group of pixels classes were identified. The n-Dimensional Visualizer allows us to rotate the data interactively in the n-Dimensional space and selection of clusters of pixels into different classes [Boardman, J. W. 1998]. The spectra of the end members which is extracted it essential to examine and compare them with the standard library spectra to assign these end members to specific mineral types and the selected end members are stored in an ASCII file for further processing.

3.6 Spectral Angle Mapper

Spectral angle mapper is very widely used as measure for spectral similarity and it is good methods for classification of the hyperspectral images. It determines the similarity between library spectra and image spectra by calculating the angle between the both spectra and treating them as a vector in n-dimensional space where the n is equal to the number of bands it is quite similar to supervised classification method used for multispectral image classification. It is a procedure that determines the similarity between a pixel and each of the reference spectra based on the calculation of the “spectral angle” between them. The angle between the two spectrums is the key to measure the difference between these two spectra

Smaller angular difference determines more similarity and large angular difference shows less similarity between image spectra and reference spectra. Let us consider the image spectrum as (t) and reference spectra (r) and the difference between the angle is (θ) for each channel (i) [Van der Meer, 2003].

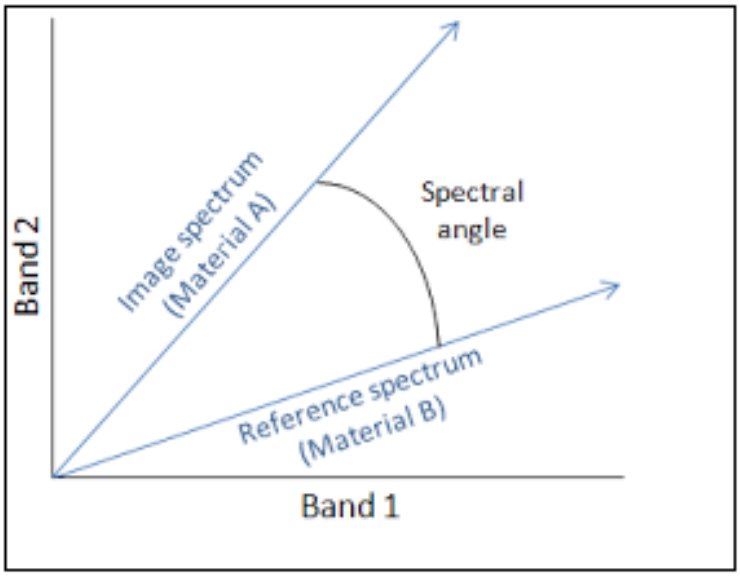

Figure: 2 Spectral Angle Mapper

$$\theta = \cos^{-1}\left[\frac{\sum_{i=1}^{n} t_i r_i}{\left(\sum_{i=1}^{n} t_i^2\right)^{1/2}\left(\sum_{i=1}^{n} r_i^2\right)^{1/2}}\right]$$

Where,

r = reflectance spectra
t = unknown spectra
n =number of bands

The algorithms like spectral feature fitting and mixture tune matched filter can also be used for per pixel and sub pixel classification. SAM is one of the best methods for hyperspectral image classification and it is similar to supervised classification method used for multispectral images. It deals equally with all possible illumination. As the spectra is transformed into vector, hence only the direction of the vector is considered and not their magnitude The figure [3] represents the standard set of procedure for hyperspectral image analysis in mineral identification and abundance mapping.

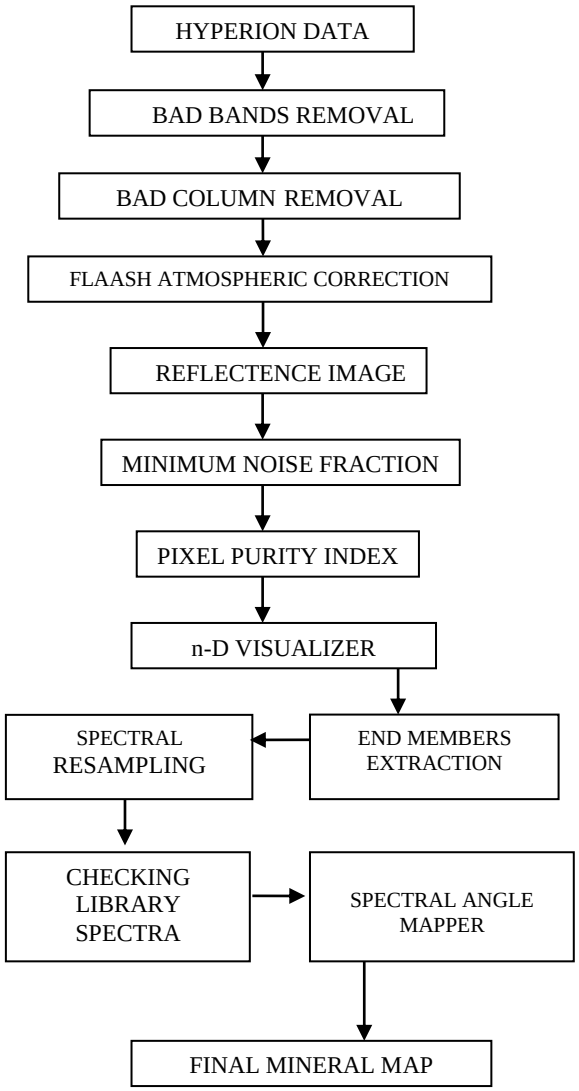

Figure: 3 workflow for hyperspectral data processing

4 RESULTS AND DISCUSSION

The preprocessing was performed to identify and remove bad bands and bad columns from the image. The bad columns were identified by examining each band individually and removed by replacing with the average of adjacent columns The FLAASH atmospheric correction tool was used with required information to compensate the atmospheric effects and to convert the radiance into apparent reflectance. The forward MNF transformation was performed on 160 bands of the atmospherically corrected image to reduce the data dimensionality. Figure [4] shows the Eigen value plot for the MNF transformed bands, where the values after the first fifteen Eigen bands were selected containing minimum noise and most of the spectral information. the rest of the bands were not considered for further processing as they contains maximum noise and their Eigen values were around one.

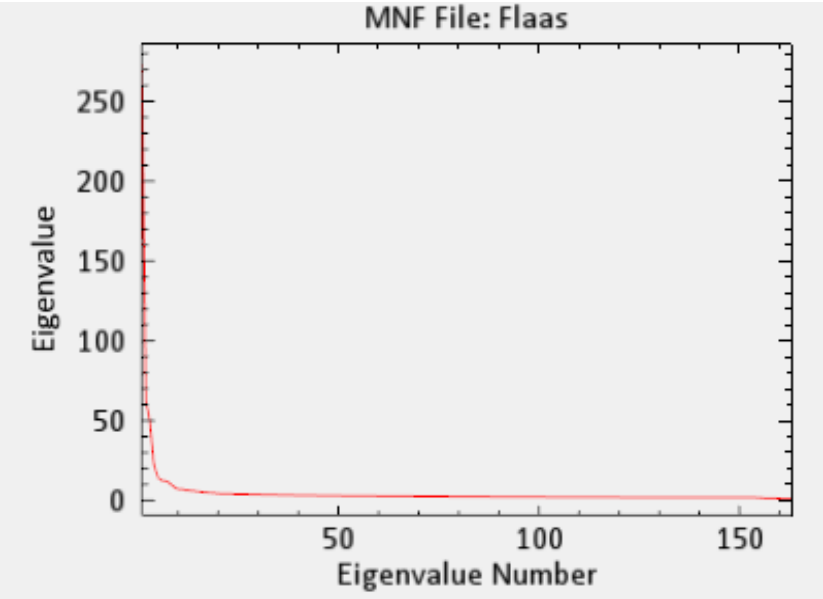

Figure: 4 Plot for MNF Eigen Values

The PPI algorithm then applied on the fifteen noise free MNF bands to identify the spectrally pure pixels. PPI was calculated with 10000 iterations and a threshold factor of 2.5 for extreme pixel identification. From the PPI image in figure [5]. The purest pixels were selected by giving a threshold of higher minimum threshold as 100. A total of 900 pixels were selected to create a region of interest (ROI). These pixels were used for end member extraction using n-dimensional visualizer. The spectra of pure pixels were plotted into an n-dimensional scatter plot to determine the end members.

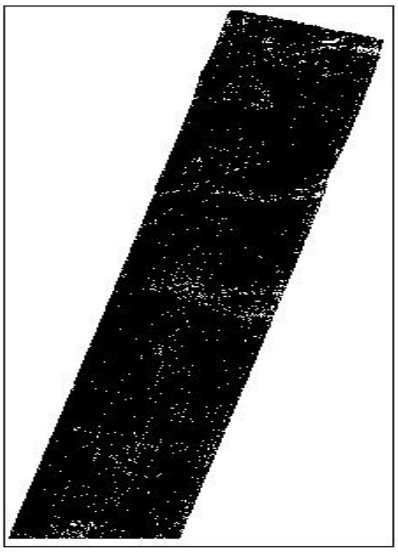

Figure: 5 PPI Image

The USGS mineral library was used due to lack of field spectrometer data through spectral analyst and the endmembers for material identification are extracted as different classes using the n-dimensional visualizer. Figure [6] shows the endmembers identified using the spectral analyst tool in ENVI software. The Spectral Angle Mapper algorithm was used for the identification. The mineral with maximum score for matching was identified as the material for that endmember. The group of pixels for each material were analyzed finalized by examining the spectral profiles of each pixel in the group. Finally three minerals were identified through the process and they are Nontronite, Richterite and Andradite.

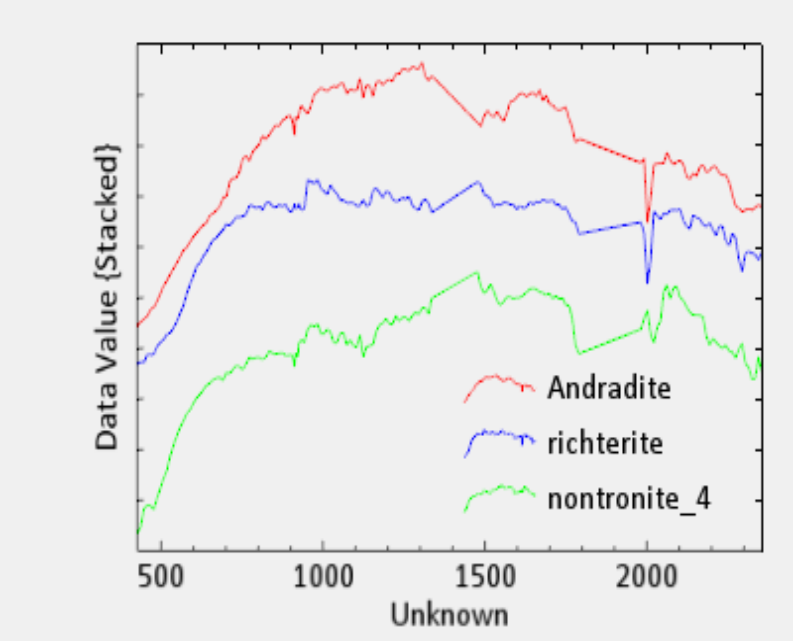

Figure: 6 Profile of End member spectra

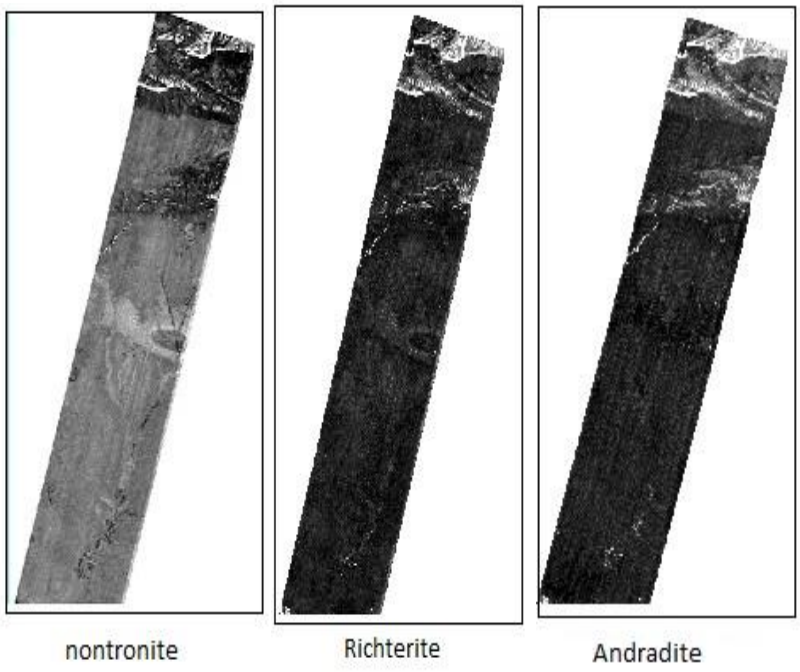

Figure: 7 Mineral abundance maps for Andradite, Richterite and Nontronite.

5 CONCLUSION

Hyperion data analysis for mineral identification over Badush area in Iraq has illustrates the use of hyperspectral data for surface mineral identification and mapping. The hyperspectral image has been analyzed using standardized set of procedures consisting of pre-processing atmospheric correction, end member extraction and the use of standard reference USGs libraries for mineral identification and mapping. Because of certain limitation however

ground truth cannot be done but the obtained results show the potential use of hyperspectral data for surface mineral identification and mapping.

REFERENCES:

S.S.S., Upadhyay R, Srivastav S.K. and Prabhakaran, Mineral Abundance Mapping Using Hyperion Dataset in Part of Udaipur Dist Rajasthan, India, Indian Geospatial Forum, (2012)

Boardman, J.W., Kruse, F.A. (1994). Automated spectral analysis: A geologic example using AVIRIS data, north Grapevine Mountains, Nevada: in proceedings, Tenth Thematic conference on geologic remote sensing, Environmental research institute of Michigan, Ann Arbor.

Green, A.A., and Craig, M.D. (1985), Analysis of aircraft spectrometer data with logarithmic residuals (abs): in proceedings, AIS work shop, 8-10 April, 1985, JPL publications 85-41, Jet Propulsion Laboratory, Pasadena, California.

Boardman, J. W., Kruse, F. A., and Green, R. O., 1995, Mapping target signatures via partial unmixing of AVIRIS data: in Summaries, Fifth JPL Airborne Earth Science Workshop, JPL Publication 95-1, v. 1, p. 23-26.

Boardman, J. W., 1998, leveraging the high dimensionality of AVIRIS data for improved sub-pixel target unmixing and rejection of false positives: mixture tuned matched filtering, in: Summaries of the Seventh Annual JPL Airborne Geoscience Workshop, Pasadena, CA, p. 55.

Van der Meer, F. and De Jong, S., 2003. Imaging Spectrometery. Basic Principles and Prospective Applications, 4. Kluwer Academic Publishers, Dordrecht/ Boston/ London, 35 pp.

Sharma Kiran Kumari, Chakravarty Debashish, Das Pulakesh and Bandhopadhyay Hyperion Image Analysis for Iron Ore Mapping in Gua Iron Ore Region, Jharkhand, India Jatisankar 496–499 *International Research Journal of Earth Sciences* ISSN 2321–2527 Vol. 2(9), 1-6, October (2014).

ENVI Tutorials," Research Systems, Inc., Boulder, 2002

Gupta et al. (1981). Lithostratigraphic map of Aravalli region, Southeastern Rajasthan and northern Gujarat, Geol. Surv. Ind., Hyderabad.

Bhattacharya S. et al., "Utilization of Hyperion data over Dongargarh, India, for mapping altered/weathered and clay minerals along with field spectral measurements," Int. J. Remote Sens.. 33, (17), 5438 –5450 (2012). 0143-1161.